Measurement and Prediction of Pressure Drop in Pneumatic Conveying: Effect of Particle Characteristics, Mass Loading, and Reynolds Number

Kimberly H. Henthorn,*,† Kinam Park,‡ and Jennifer S. Curtis†

School of Chemical Engineering and Departments of Pharmaceutics and Biomedical Engineering, Purdue University, West Lafayette, Indiana 47907

This paper reports the effect of Reynolds number, mass loading, and particle shape and size on pressure drop in a vertical gas−solids pneumatic conveying line. We isolate the effect of one variable while holding all others constant. A commonly used pressure drop correlation and a state-of-the-art multiphase computational fluid dynamics (CFD) models are then assessed by comparing their predictions to experimental data. Deficiencies in the models and the correlation are identified, and possible modifications are proposed. The most notable deficiency is the inability of both the experimental correlation and the CFD model to accurately predict the pressure drop for gas−solids flow with highly aspherical particles.

Background

Experimental Data and Correlations for Pressure Drop. Total pressure drop in a vertical two-phase conveying system is often estimated via experimental correlation by summing contributions from both the solid and the gas phases. Correlations typically express the total pressure drop as a sum of six terms: the acceleration of gas (1), the acceleration of solids (2), gas friction (3), solids friction (4), the weight of solids (5), and the weight of gas (6).[1,2]

$$\Delta P_T = \underset{(1)}{\frac{1}{2}\epsilon\rho_g U_g^{\,2}} + \underset{(2)}{\frac{1}{2}(1-\epsilon)\rho_p U_p^{\,2}} + \underset{(3)}{\frac{2f_g\rho_g U_g^{\,2}L}{D}} + \underset{(4)}{F_{pw}L} + \underset{(5)}{\rho_p L(1-\epsilon)g\sin\theta} + \underset{(6)}{\rho_g L\epsilon g\sin\theta} \quad (1)$$

where θ represents the angle of inclination of the pipe, U_p is the interstitial particle velocity, U_g is the interstitial gas velocity, D is the pipe diameter, L is the length over which the pressure measurement is made, ϵ is the void fraction, and F_{pw} is the solids-pipe friction force [force/length^3].

Gas friction is generally assumed to be independent of the presence of solids, so term (**3**) uses the Fanning friction factor, f_g, of single-phase pressure drop calculations. For dilute flow, it is often assumed that the slip velocity is equal to the terminal velocity, U_t, of the particles so that the void fraction can be estimated given a known solids mass flux.

$$m = \frac{(U_g - U_t)(1-\epsilon)\rho_p}{U_g\epsilon\rho_g} \quad (2)$$

where m represents the mass loading, defined to be the ratio of the mass flow rate of particles to the mass flow rate of gas. The solids friction force, F_{pw}, is the most difficult term to estimate, and numerous groups have proposed expressions based on experimental measurements. Typically, the solids friction force is described in terms of a solids friction factor, f_p, where

$$F_{pw}L = \frac{2f_p\rho_p(1-\epsilon)U_p^{\,2}L}{D} \quad (3)$$

One of the most commonly employed correlations by Konno and Saito,[3] applied in this paper, uses experimental data to determine f_p as a function of the interstitial particle velocity and the pipe diameter, resulting in the following expression for F_{pw}:

$$F_{pw}L = 0.057m\rho_g U_g\sqrt{\frac{g}{D}}L \quad (4)$$

The experiments of Konno and Saito (as well as many others including Singh,[4] Rautiainen et al.,[5] Hettiaratchi et al.,[6] and Namkung and Cho[7]) show an increase in pressure drop with increasing mass loading and Reynolds number. However, as Marcus et al.[8] and Klinzing[9] have pointed out, it is well known that for finer particles (20−75 μm) at mass loadings between 0.5 and 4.0 and Reynolds numbers between 15 000 and 40 000, pressure drop may initially decrease with increasing solids loadings at very low loadings. Interactions between particles and turbulent eddies lead to a reduction of gas-phase stress and a resulting decrease in pressure drop.

In the experiments of Konno and Saito, several different sized glass and copper spheres were used, but because the results were combined into one data set, assessment of the effect of particle size on pressure drop was not possible to determine from their data. However, by examination of the data of Nieuwland et al.[10] for glass spheres between 275 and 655 μm, pressure drop increased with increasing particle size. Plasynski et al.[11] also explored the particle size effect during high-pressure pneumatic conveying using glass spheres ranging in size from 97 to 545 μm. They concluded that pressure drop increases with increasing particle size at elevated pressures; however, the differences in pressure

* To whom correspondence should be addressed. Tel.: (573) 341-7633. Fax: (573) 341-4377. E-mail: henthork@umr.edu.
† School of Chemical Engineering.
‡ Departments of Pharmaceutics and Biomedical Engineering.

10.1021/ie049505e CCC: $30.25
Published on Web 12/10/2004

drop taken at atmospheric pressure were very small for the two particle sizes. Plasynski et al. also compared the glass sphere results to pressure drop data from two different sizes of coal particles having a density approximately half that of the glass. As expected, they concluded that measured pressure drop is generally higher for particles with greater density. Pelegrina[12] examined the effect of particle size via a one-dimensional plug flow model based on interstitial gas and solids momentum balances which described particle-wall friction using a correlation for f_p given by Yang.[13,14] From his model, Pelegrina concluded that pressure drop for spheres would increase with decreasing particle size at high Reynolds number (~31 500) because the solids friction and drag increase for smaller particles; this result contradicts the previously cited work.

Wang et al.[15] focused on the effects of smaller particles, 20 and 66 μm glass spheres, on pressure drop. Solid-phase friction factors, f_p, were deduced from overall pressure drop measurements and compared to results from three published friction factor correlations.[3,13,14,16] In all cases, the experimental data for pressure drop were much lower than the predictions over a range of mass loadings from 5 to 20. Wang et al. attributed this difference to the cohesiveness of the powder. They proposed that interactions with the pipe wall are much more prominent for cohesive material so that as the particles are conveyed, some particles will deposit on the wall and others will be re-entrained by the gas. As a result, a lubrication effect associated with the particle−wall collisions may be occurring, resulting in a lower friction factor. Their data also showed that as the Reynolds number increases at low mass loadings, the pressure drop decreases, but at higher mass loadings, the pressure drop increases with increasing Reynolds number. Additionally, the pressure drop increases with increasing particle size at higher Reynolds numbers (>12 500) but decreases with increasing particle size at lower Reynolds numbers.

Pelegrina[12] also examined the effect of particle shape with particles of the same equivalent volume diameter using his one-dimensional plug flow model. Experimental settling data for particles with sphericities ranging from 0.72 to 1.0 were correlated from the work of others[17,18] to yield a relationship between the particle drag coefficient as a function of the particle Reynolds number, the particle sphericity ϕ, and the particle shape factor for momentum transfer−defined as the ratio of the projected area of the equivalent sphere to the real projected area of the particle. He found that the pressure drop is higher for nonspherical particles as compared to spheres having the same volume; he attributed this result to the increase in projected area and drag for nonspherical particles. This result was in agreement with what Hariu and Molstad[19] found from direct experimentation measuring pressure drop for gas−solids flow in a riser with spherical and nonspherical catalyst particles having the same sieve diameter ranging from 177 to 590 μm.

Haider and Levenspiel[20] developed a drag coefficient, C_d, correlation for nonspherical particles based on experimental sedimentation data with a wide variety of particle sphericities from numerous groups. The particle Reynolds numbers, Re_p, of the experimental data ranged from approximately 0.01 to 250 000.

$$C_d = \frac{24}{Re_p}(1 + A\,Re_p^{\,B}) + \frac{C}{1 + \frac{D}{Re_p}} \tag{5}$$

where

$$A = \exp(2.3288 - 6.4581\phi + 2.4486\phi^2) \tag{6}$$

$$B = 0.0964 + 0.5565\phi \tag{7}$$

$$C = \exp(4.905 - 13.8944\phi + 18.4222\phi^2 - 10.2599\phi^3) \tag{8}$$

$$D = \exp(1.4681 + 12.2584\phi - 20.7322\phi^2 + 15.8855\phi^3) \tag{9}$$

Drag coefficients for particle sphericities ranging from 0.806 to 1.0 displayed good fit when compared to the correlation; tetrahedron-shaped particles having a sphericity of 0.670 also showed fairly good agreement. In addition, disks with sphericities ranging from 0.026 to 0.23 were studied; the fit between the experimental data and the correlation was much poorer in this case. For the most aspherical particle considered by Pelegrina[12] ($\phi = 0.72$), over a particle Reynolds number range from 1 to 30, the Haider and Levenspiel drag coefficient correlation is approximately 70−85% higher than the drag coefficient as given by Pelegrina. It should be noted that almost all of the particles discussed in these two papers were more spheroidal in shape than the particles used in the current work; as a result, the drag coefficient expressions discussed in this paper may not be appropriate for the range of sphericities investigated here.

Gas−Solid Computational Fluid Dynamics (CFD) Models. As computer capacity has increased, the development of CFD models has grown at a rapid pace. Models such as the works of Arastoopour and Gidaspow,[21] Nakamura and Capes,[22] and Nieuwland et al.[10] describe the gas−solid system in a two-fluid framework and allow for pressure drop variations along the axial length of the tube. Particle-phase stresses are described empirically, and an additional force term is added to the balance of momentum for the particle phase. Other models such as the work of Chen and Marshall[23] describe the particle motion in a detailed fashion via a Lagrangian treatment and account for particle−particle and particle−wall collisions. These models, however, are limited to solids loadings which are much more dilute than the range of loadings considered in this work unless an assumption of a fictitious "particle packet" is employed.

Models that allow for solid density variations over the tube cross section and describe particle−particle collisions in a fundamental way stem from the seminal work of Sinclair and Jackson,[24] whose model is based on the two-fluid framework of Anderson and Jackson.[25] Sinclair and Jackson's model utilized kinetic theory concepts to describe the stresses associated with the particle−particle and particle−wall interactions, assuming that the random motion of particles in a gas−solids system resembles that of molecules in a gas.

Louge et al.[26] incorporated the work of Sinclair and Jackson into their model but extended its applicability to a turbulent gas. They also accounted for the effect the two phases have on one another at the level of the velocity fluctuations. Bolio et al.[27] further developed the Louge et al. model by adding a $k-\epsilon$ model to describe

gas turbulence that is modified for the presence of a dilute particle phase. In this model, three terms from the gas momentum balance sum to give the total pressure drop: the weight of the gas (term 4, eq 10), gas-phase stress estimated through a modified $k-\epsilon$ model (term 3, eq 10), and drag (term 2, eq 10).

$$0 = \underset{(1)}{-\frac{\partial p}{\partial z}} - \underset{(2)}{\beta(U_{gz} - U_{pz})} + \underset{(3)}{\frac{1}{r}\frac{\partial}{\partial r}\left[r(\mu + \mu_t)\frac{\partial U_{gz}}{\partial r}\right]} - \underset{(4)}{\rho_g(1-\nu)g} \quad (10)$$

where β is the drag coefficient, ν is the particle volume fraction, and μ_t is the eddy viscosity. Drag can be found via the axial solid-phase momentum balance (axial component eq 11; radial component eq 12) by summing the weight of the particles (term 3, eq 11) and the solid-phase stress (term 1, eq 11).

$$0 = \underset{(1)}{-\frac{1}{r}\frac{\partial}{\partial r}(r\sigma_{rz})} + \underset{(2)}{\beta(U_{gz} - U_{pz})} - \underset{(3)}{\rho_p \nu g} \quad (11)$$

$$0 = -\frac{1}{r}\frac{\partial}{\partial r}(r\sigma_{rr}) - \frac{\sigma_{\theta\theta}}{r} \quad (12)$$

where σ_{rz} and σ_{rr} are the solid-phase stress tensors as given by the kinetic theory of Lun and Savage.[28]

Hadinoto and Curtis[29] have recently extended the model of Bolio et al. to account for lubrication effects in particle−particle collisions. They recognized that the behavior of collisions in a vacuum as described by the kinetic theory of Lun and Savage, characterized by a coefficient of restitution e_s, can be significantly different than that for particles colliding in a viscous fluid, characterized by a coefficient of restitution e_f, where e_f is less than e_s. They have shown improved predictions for gas−solids flow in the case of smaller particles (less than 100 μm) and very good predictions for liquid−solid flow with large Bagnold numbers (collision-dominated flows). In the case of large particles in a gas, their predictions asymptote to the results given by the Bolio et al. model.

The Hadinoto and Curtis gas−solid flow model is the CFD model employed in this paper for comparison with experimental data for the pressure drop. In the previous paper (Hadinoto and Curtis[29]), comparisons of the model predictions with Laser Doppler velocimetry (LDV) data were made for radial profiles of the mean gas velocity, mean solids velocity, fluctuating gas velocity, and fluctuating solids velocity. While pressure drop comparisons are not as detailed as radial profile comparisons, the pressure drop comparisons nevertheless indicate whether the model is performing well at the macroscopic level. Also, in this paper, a wider range of particle sizes and shapes are employed than in the previous paper. In addition, the use of pressure drop data enables comparisons between CFD model predictions and predictions from the correlation.

Particle-phase slip at solid boundaries is described following Sinclair and Jackson.[24] The particle-phase slip is a function of the fraction of tangential momentum lost at the wall, represented by a specularity coefficient, ϕ ($0 < \phi < 1$), which depends on the wall roughness. The granular energy at the wall is found by equating the flux of granular energy to the wall to the sum of the energy lost at the wall by inelastic particle−wall collisions (which depends on the coefficient of restitution for particle−wall collisions) and the energy gained by particle shearing at the wall due to slip.[24]

This paper reports the effect of Reynolds number, mass loading, and particle shape and size on pressure drop in a vertical gas−solids pneumatic conveying line. The effect of one variable is investigated while holding all others constant. The Konno and Saito[3] pressure drop correlation and the Hadinoto and Curtis (2004) multiphase CFD model are then assessed by comparing their predictions to experimental data.

Experimental Section

A schematic of the vertical conveying line system is shown in Figure 1. Pressurized air was filtered of oil and moisture before moving through a series of pressure regulators and flow measuring devices. Air velocity increased as the air passed through a 2 mm diameter Venturi feeder, which aided in entrainment of particles coming from the attached hopper. A bypass line was added to pressurize the hopper so that higher particle flow rates could be achievable. The particle-laden air then flowed through a smooth 90° elbow to a vertical 1 in. diameter copper tube, which was grounded to reduce electrostatic effects. Fully developed turbulent flow is expected to form in a 50 in. development length given the low solids loadings. Two pair of water manometers, sensitive to ±0.001 in. of H_2O, indicated that the pressure drop was not changing with axial distance. (It should be noted that there was a slight degree of oscillation in the pressure readings. The degree of oscillation in the pressure readings varied with the solids loading, from a negligible amount at the lower loadings to occasional pressure drop increases of up to 25% of the base pressure drop value. It is hypothesized that the occasional pressure increases were associated with occasional clusters of particles passing through the system.) Pressure drop was measured over an 8 in. vertical section of pipe, after which the particle-laden air flowed through another smooth elbow to the filtration section. Particles were removed from the gas stream using a cyclone separator, and the mass flow rate of solid was measured by using a scale to continuously weigh the captured particles. The scale used in the process is accurate to ±0.1 lb. On average, pressure drop measurements were repeated three times, and the mean value was reported in the Results and Discussion section. Error bars on the graphs in the results section indicate the maximum deviation from mean value associated with these repeated measurements. From a detailed error analysis,[30] the errors in the reported mass loading and Reynolds number are 9% and 6%, respectively.

Properties for the particles used in the experiments are shown in Table 1. The standard deviation of the particle sizes is approximately 20% of the reported mean value. The sphericity of the particles was determined by measuring the pressure drop through a packed bed and employing the Carman−Kozeny equation to relate the pressure drop to particle sphericity. The uncertainty associated with the sphericity measurements was approximately 14%.[30] The glass particles have a sphericity close to 1; the sand and mica are highly nonspherical. The mica particles are flakes, and the sand particles are both spheroidal and platelike in shape as evidenced by scanning electron microscopy (SEM) photographs (Figure 2). All particles were dried for at least 3 days

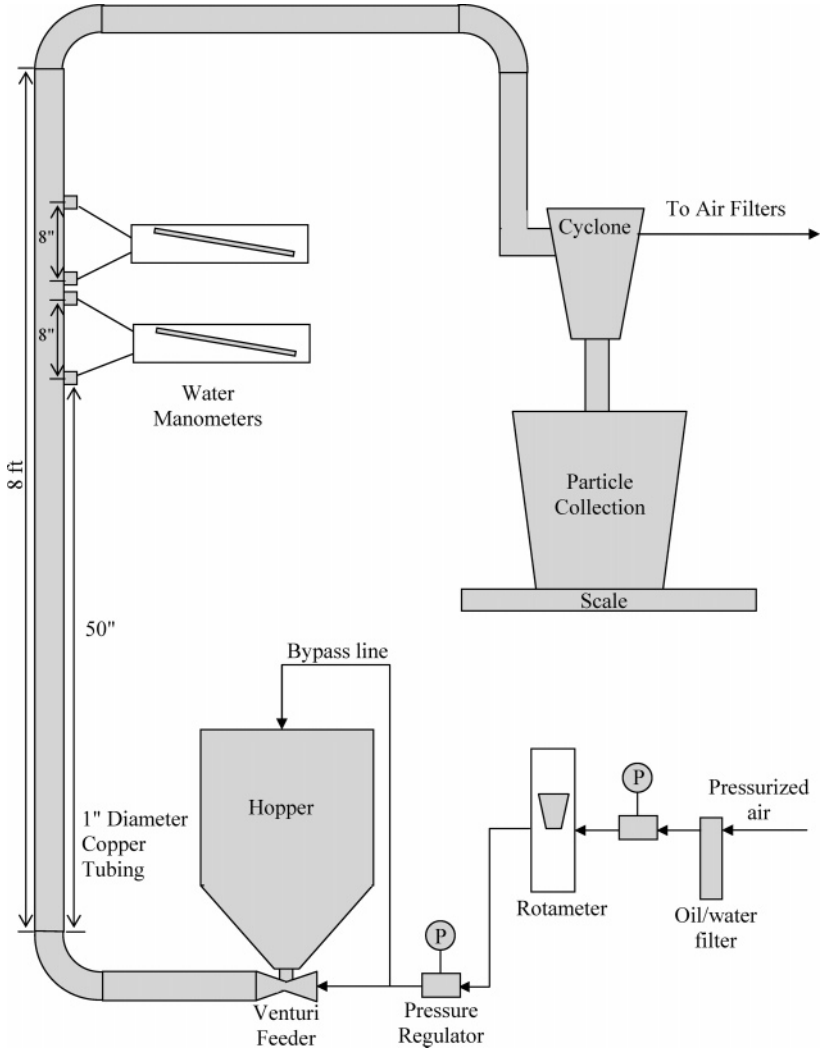

Figure 1. Experimental setup for measurement of pressure drop.

Table 1. Properties of Particles Used in the Experiments

particle type	density (g/cm^3)	mean equivalent volume diameter (μm)	sphericity
glass	2.5	70	0.97
		200	
		275	
		500	
sand	2.6	154	0.59
		260	
mica	2.8	154	0.64
		260	0.39

in a drying oven and stored in a desiccator to minimize the presence of moisture in the system.

The coefficient of restitution for particle−particle collisions, e_s, is 0.94 and representative of collisions between glass beads.[31] The coefficient of restitution for particle−wall collisions, e_w, is 0.15 and representative of collisions between glass and copper (the pipe wall material).[31] A value for e_f, the coefficient of restitution for particle−particle collisions accounting for the viscosity of the interstitial fluid, is found based on the work of Gondret et al.[32] They showed that the ratio of e_f to e_s is a function of the impact Stokes number, defined as

$$St = \frac{m_p v_{imp}}{6\pi\mu_g d_p^2} \tag{13}$$

where m_p is the particle mass and v_{imp} is the impact velocity of the particle. For glass beads flowing in air at the velocities considered in this work, the value for e_f is 0.93. For all of the gas−solid systems considered in this work, the value of e_f is very close to e_s because the impact Stokes number is very high (>1200) due to the low viscosity of the fluid and the large particle velocities. A sensitivity analysis of the predicted pressure drop as a function of e_f, holding the ratio of e_f to e_s constant and at a mass loading of 2.0, revealed that a 26% change in e_f produced less than a 7% change in predicted pressure drop. Hence, the model predictions for all particles investigated were obtained with a value of $e_s = 0.94$ and $e_f = 0.93$. In addition, the sensitivity of pressure drop with respect to e_w was also investigated. For 70 μm glass spheres at a Reynolds number of 20 400 and a mass loading of 0.5, changing the value of e_w from 0.15 to 0.135 produced a negligible change in predicted pressure drop. Hence, the model predictions for all particles reported in this paper were obtained with a value of $e_w = 0.15$. The specularity coefficient was held constant at 0.008 for all predictions, which is representative of the wall roughness associated with a copper pipe. This was determined previously by comparisons between model predictions and pressure drop data obtained in a copper pipe[33] and comparisons between model predictions and LDV data obtained in a copper pipe.[29]

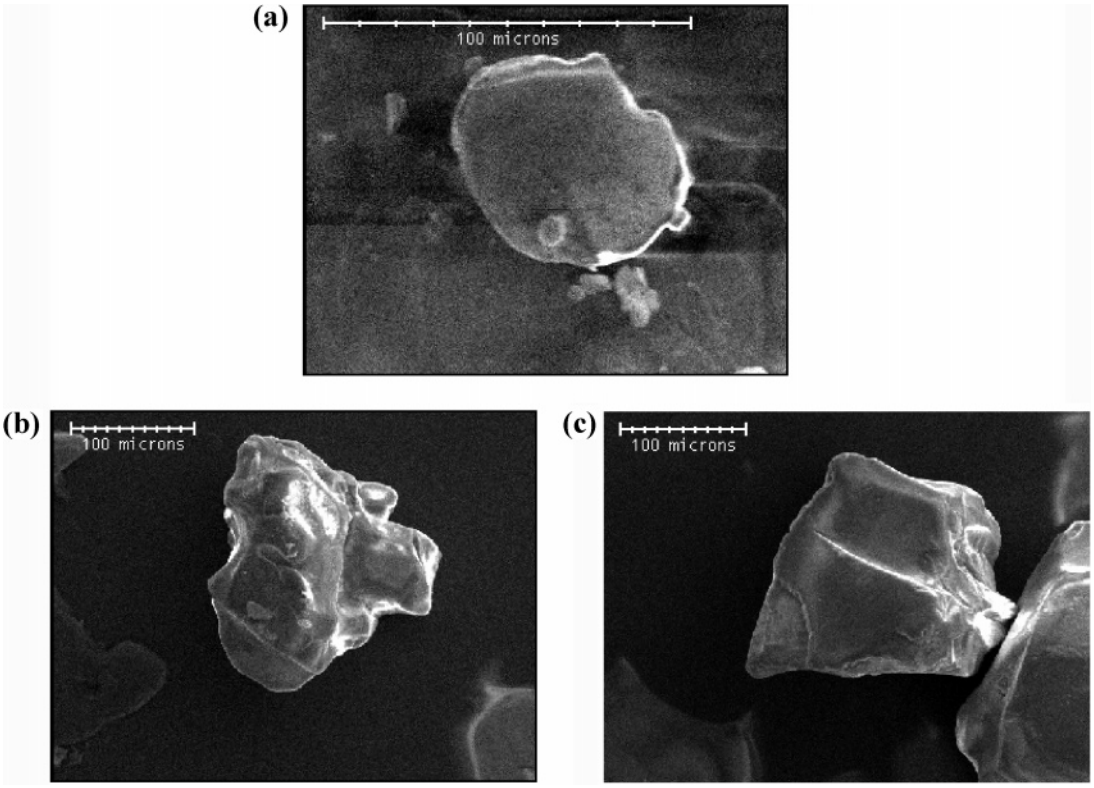

Figure 2. SEM images of (a) mica flake, (b) spheroidal sand particle, and (c) flat sand particle.

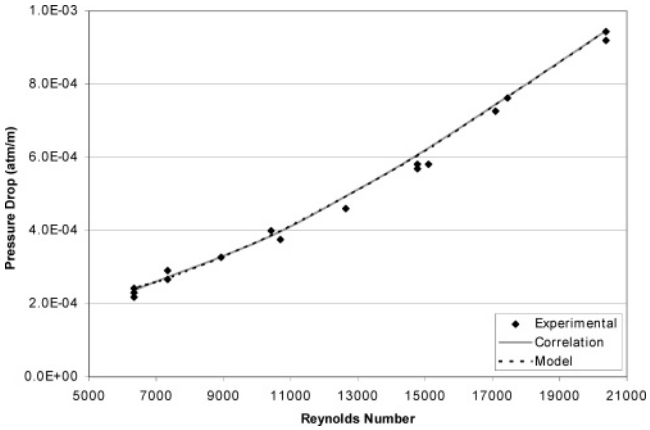

Figure 3. Comparison of single-phase pressure drop determined by the Hadinoto and Curtis[26] model, correlation, and experimental data.

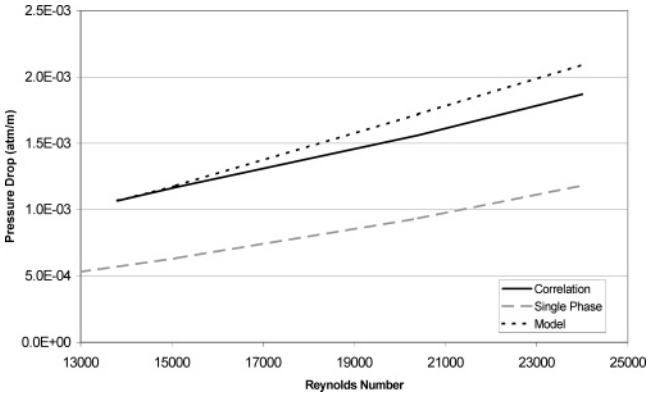

Figure 4. Pressure drop predictions made by the Hadinoto and Curtis[26] model and Konno and Saito[3] correlation for two-phase flow at $m = 2.0$ and $d_p = 70$ μm.

Results and Discussion

Experimental pressure drop measurements were first collected for single-phase flow over a range of Reynolds numbers from 6300 to 20 300. These data were compared with single-phase predictions based on the single-phase fanning friction factor and the Hadinoto and Curtis[29] model. Agreement between measurement, correlation, and model prediction is excellent (see Figure 3).

Reynolds Number Effects. Figure 4 shows pressure drop predictions made by the Hadinoto and Curtis model and the experimental correlation of Konno and Saito[3] for the 70 μm particles at a constant mass loading of 2.0 over a range of Reynolds numbers. Differences between the two predictions can be studied through inspection of the four terms contributing to the overall pressure drop. The gas gravity term is in fairly good agreement between the correlation (term 6, eq 1) and model (term 4, eq 10). The correlation predicts a much higher (~114%) gas-phase stress (term 3, eq 1) than the model (term 3, eq 10) over the entire range of Reynolds numbers. This difference is because the correlation neglects any direct effect of the particles on the gas-phase stress while the model predicts damping of gas-phase turbulence in the presence of the 70 μm particles. (LDV) data[34] for the same system (solids loading = 0.7) indicate that the prediction of turbulence damping is indeed accurate for lower Reynolds numbers but some turbulence enhancement is seen near the pipe centerline at higher Reynolds numbers (Figure 5), which is not captured by the model. In Figure 5, the open symbols represent gas-phase velocity fluctuations in particle-laden flow, and the closed symbols represent gas-phase velocity fluctuations in single-phase flow. The uncertainty associated with the LDV measurements is approximately 9% for gas-phase velocity fluctuations (U') in particle-laden flow and 8% for single-phase gas velocity fluctuations.[29] The model predicts a much

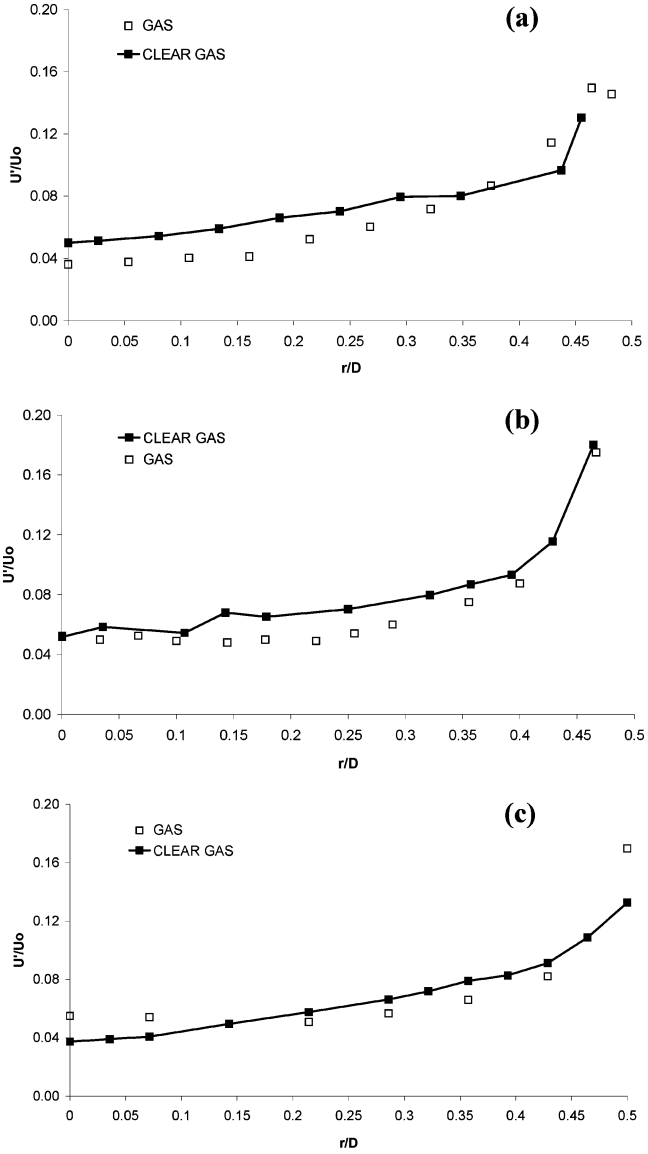

Figure 5. LDV data for (a) $Re = 8300$, (b) $Re = 13\,800$, and (c) $Re = 20\,800$.[31]

higher (~71%) solid-phase stress (term 1, eq 11) than the correlation (term 4, eq 1) at higher Reynolds numbers, but the correlation predicts a higher solid-phase stress for Reynolds numbers less than 20 400. However, the magnitude of the solid-phase gravity term in the model (term 3, eq 11) relative to the correlation (term 5, eq 1) increases with decreasing Reynolds number. This is because the correlation shows a negligible dependence of solid-phase gravity on Reynolds number, but the model predicts that the solid volume fraction increases as the Reynolds number decreases, resulting in an increase of the solid-phase gravity term with decreasing Reynolds number. The overall effect for 70 μm particles is a higher overall pressure drop prediction by the Hadinoto and Curtis model for Reynolds numbers greater than 13 800. These trends are the same for the 200 μm particles but much less pronounced, resulting in comparable pressure drop predictions for the model and correlation.

Two-phase pressure drop measurements were obtained over a Reynolds numbers range of 12 600 to 20 400. In the present conveying system with 70 μm glass spheres, a Reynolds number of 12 600 is required

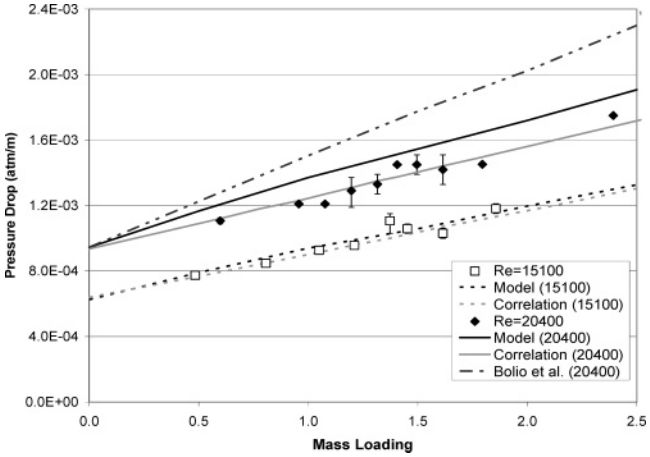

Figure 6. Comparison of experimental data to the Hadinoto and Curtis[26] model, Bolio et al.[24] model, and Konno and Saito[3] correlation for 70 μm glass spheres.

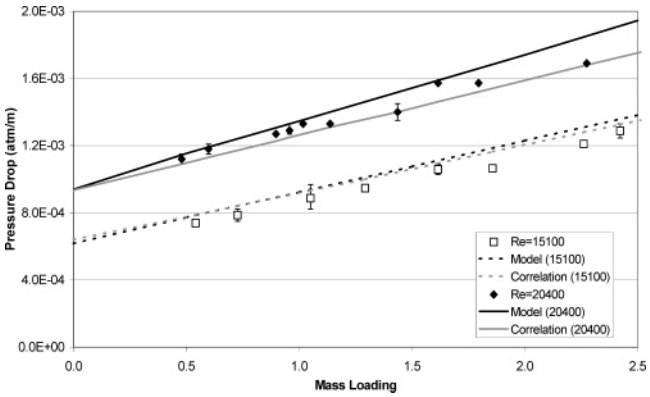

Figure 7. Comparison of experimental data to the Hadinoto and Curtis[26] model and Konno and Saito[3] correlation for 200 μm glass spheres.

for particle pickup velocity. In addition, limitations of the equipment prevent achieving Reynolds numbers higher than 20 400. The data (Figures 6 and 7) indicate that, holding all other variables constant, absolute pressure drop increases with increasing mass loading and Reynolds number, which is in agreement with the trends observed in the literature for particles in the size range considered in this study.

Figure 6 compares experimental pressure drop measurements to the predictions from the Hadinoto and Curtis model and to the experimental correlation for 70 μm glass spheres at Reynolds numbers of 15 100 and 20 400. Also shown are the predictions of the Bolio et al.,[27] model which significantly overpredict the pressure drop. The correlation is able to capture the pressure drop well at both Reynolds numbers, but some deviations (approximately 10%) between the experimental data and the values predicted by the model are apparent at the higher Reynolds number. Examination of the model contributions to the predicted pressure drop reveals that both the gas-phase stress and the solid-phase stress slightly increase as the Reynolds number is increased. However, because the LDV measurements in Figure 5 show that gas-phase eddy viscosity is underpredicted at higher Reynolds numbers, the overprediction in the pressure drop must be due to inaccuracies in the contribution from the solid-phase stress. Hence, the model is not completely capturing the decrease in the solid-phase momentum flux due to the effect of lubrication. The lower pressure drop measure-

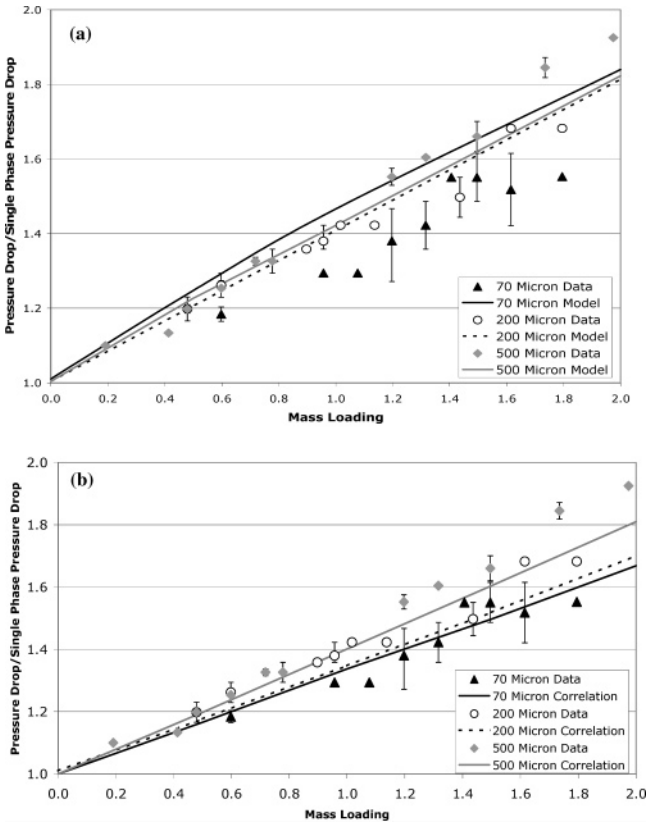

Figure 8. Particle size effects for glass spheres at $Re = 20\,400$. Comparison of data to (a) the Hadinoto and Curtis[26] model and (b) the Konno and Saito[3] correlation.

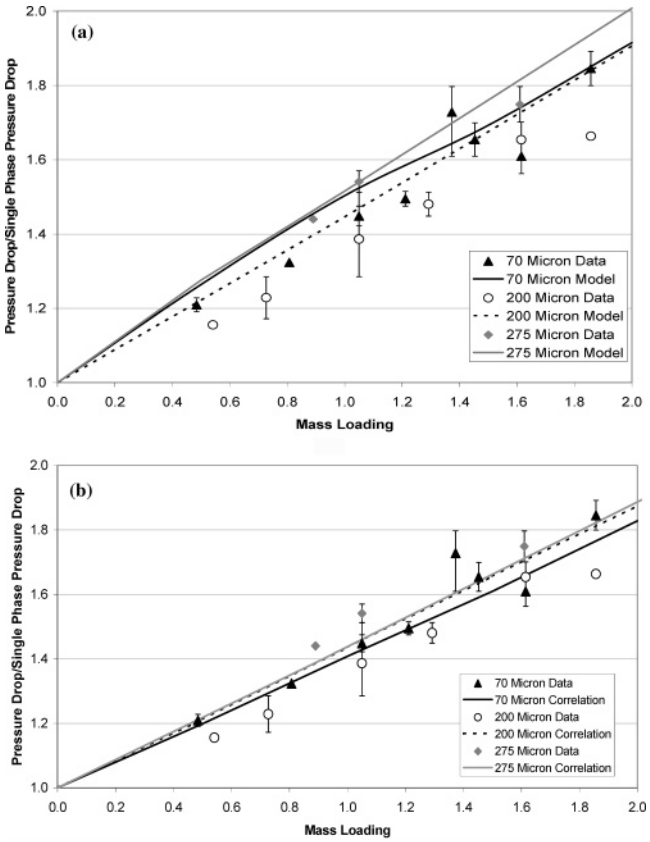

Figure 9. Particle size effects for glass spheres at $Re = 15\,100$. Comparison of data to (a) the Hadinoto and Curtis[26] model and (b) the Konno and Saito[3] correlation.

ments with these finer particles could also be due to the phenomenon that Wang et al.[15] observed, finer glass bead particles depositing on the pipe wall, an effect not described in the CFD model.

The pressure drop predictions with 200 μm glass beads, shown in Figure 7, indicate that both the model and the correlation are able to accurately capture the pressure drop. For 200 μm glass beads flowing in a gas at the range of Reynolds numbers considered here, the effect of lubrication on the solid-phase stress is negligible. The model clearly performs very well in this particle flow regime.

Particle Size Effects. Figure 8 illustrates particle size effects for 70, 200, and 500 μm glass spheres at a Reynolds number of 20 400. Because the Reynolds number is constant, in this and subsequent figures, the two-phase pressure drop is normalized with that of clear gas. At this Reynolds number of 20 400, the experimental data show an increase in pressure drop with increasing particle size, which agrees with the trend predicted by the correlation and the data set of Nieuwland et al.[10] However, the model predicts that pressure drop first decreases as particle size increases, and then increases with increasing particle size. The experimental data in Figure 9 appear to display the same trend with increasing particle size as predicted by the model, but at the lower Reynolds number of 15 100. (Unfortunately, the particle size range that could be investigated at the Reynolds number of 15 100 was limited by pickup velocity considerations; 500 μm glass spheres could not be conveyed at this lower Reynolds number.) The correlation is not able to predict this behavior at the lower Reynolds number of 15 100 but consistently predicts that pressure drop increases with increasing particle size. This particle size dependency in the correlation is due to the assumption that the interstitial particle velocity is always equal to the difference between the interstitial gas velocity and the particle terminal velocity. While this assumption is true for smaller, lighter particles, for the particles investigated here whose motion is significantly influenced by particle−particle and particle−wall interactions, this assumption is not accurate. LDV data, in fact, indicate that the particle velocity exceeds the gas velocity near the wall.[35,36] The experimental data shown in Figure 9 mimic the observations of Wang et al.,[15] who also observed that pressure drop decreases with increasing particle size at lower Reynolds numbers. At higher Reynolds numbers, Wang et al. found the same results as shown in Figure 8 at the higher Reynolds number of 20 400 with smaller particles (20 and 66 μm), that the pressure drop increases with increasing particle size.

Examination of contributing terms to overall pressure drop in the model explains the observed trends. At both Reynolds numbers of 15 100 and 20 400, the gas-phase and solid-phase stress terms increase and then decrease as particle size increases, but these trends are overshadowed by the solids gravity term, which decreases then increases with increasing particle size, resulting in the same trend for the overall pressure drop. However, this trend predicted by the model becomes less pronounced as the Reynolds number increases. At a Reynolds number of 15 100, the increase in pressure drop from 200 to 500 μm particles is much more significant than the increase at a Reynolds number of 20 400.

Particle Shape Effects. To study the effect of particle shape on pressure drop, experiments were

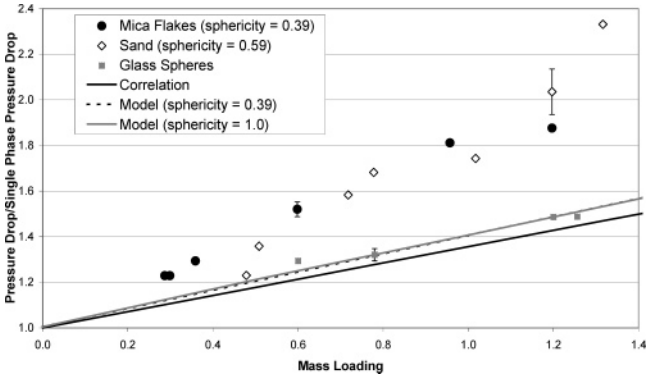

Figure 10. Shape effects for particles with an equivalent volume diameter 260 μm at $Re = 20\,400$.

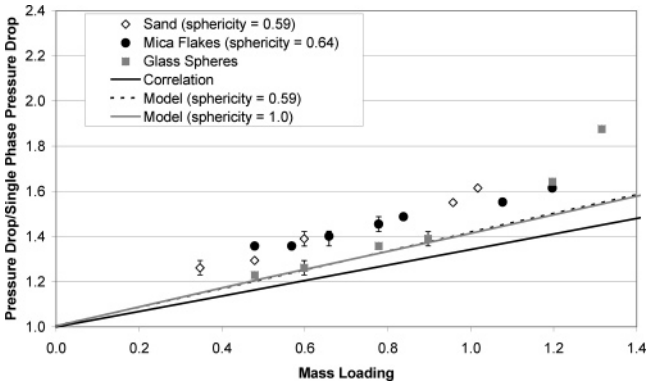

Figure 11. Shape effects for particles with an equivalent volume diameter 154 μm at $Re = 20\,400$.

performed with three types of particles having similar equivalent diameters and densities but varying in shape. Mica flakes with equivalent volume diameters of 154 and 260 μm having aspect ratios of 5 and 14, respectively, were compared to nonspherical sand of both spheroidal and platelike shapes and spherical glass spheres. Material specific gravity ranged from 2.5 for glass to 2.8 for mica, but assessment of the sensitivity of the predicted pressure drop of the model with respect to particle density revealed that this magnitude of density variation has a negligible effect on the pressure drop. Particle size is reported as equivalent volume diameter, which is defined as the diameter of a sphere having the same volume as the particle.

Figures 10 and 11 present data at a Reynolds number of 20 400 for the three particle types having equivalent volume diameters 260 and 154 μm, respectively. As expected, the model adequately predicts pressure drop over a range of mass loadings for the spherical glass particles. The correlation underpredicts the pressure drop for the spherical particles by less than 10%. However, there is a huge deviation between the measurements and the predicted values from both the correlation and the model for the two irregularly shaped materials. The deviation between the measurements and predictions increases with increasing particle diameter. In addition, the difference between experimental data taken for mica flakes and sand was negligible; the data do not show a significant change in pressure drop between these two particle types at either equivalent particle diameter.

Deviations between measurement and prediction are expected with the correlation, as the correlation has no dependency on particle shape. Also, clearly the pressure drop predictions from the model, which accounts for the effect of particle shape through the use of the Haider and Levenspiel[20] drag coefficient, are not sufficiently sensitive with respect to sphericity. As mentioned earlier, Haider and Levenspiel found that their nonspherical drag coefficient correlation predicted the measured drag coefficients well for spheroidal particles but not disklike particles. The inability of the model to capture the effect of particle shape on the pressure drop with these highly nonspherical particles may be because the drag force modification for these particles depends on more than just the sphericity. Because sphericity is a ratio of surface areas, two particles may have the same value of sphericity but behave differently in a flowing fluid because their projected areas may be radically different. In addition, particle orientation in the flowing fluid will affect the drag force, and, in turbulent flow, particles do not have a uniform orientation throughout the flow field. For example, a spheroidal particle may have the same sphericity as a flaky particle, but these two types of particles will have different orientations and different projected areas during flow and, consequently, experience different drag forces. Finally, the effect of sphericity is not accounted for in the description of the gas turbulence modulation due to the presence of the particles and in the kinetic theory of Lun et al.[37] used to describe the particle-phase stress.

Conclusions

This investigation reveals that variations in particle shape greatly affect the pressure drop measured in a vertical conveying line, particularly for highly aspherical particles. However, comparisons between the experimental data and the CFD model and the experimental correlation indicate that both the model and the correlation are currently not able to capture particle shape effects. Hence, the body of data on which the experimental correlation is based needs to be expanded to include highly aspherical particles. Also, further refinement of the model will require implementation of a drag coefficient expression for highly nonspherical particles.

The model implemented in this work utilizes the drag coefficient expression for nonspherical particles proposed by Haider and Levenspiel. However, the particle shapes studied in the current work lie outside the range of sphericities applicable for this expression. As a result, the development of a drag coefficient expression for particles having very low sphericity is needed. In addition, consideration of additional particle characteristics, such as projected area, surface roughness, fractal dimension, and particle orientation, may be necessary to develop such an expression.

Another reason the current CFD model cannot adequately capture the effect of particle shape may be due to the lack of a solids stress model for highly nonspherical particles. While no such model has been developed to date, there are presently several research groups studying collisions between nonspherical particles. Huthmann et al.[38] and Aspelmeier et al.[39] have theoretically investigated the exchange of translational and rotational energy resulting from collisions between needlelike particles. Walton and Braun[40] have used discrete element techniques and event-driven, hard-sphere collision operators to study the dry granular flow of nonspherical particles. We anticipate that the implementation of a solids stress model for nonspherical particles, in addition to incorporating a more applicable drag coefficient expression, will allow the current CFD

model to better capture the effects of particle shape observed in the experimental data.

This paper also illustrates the current lack of ability of the model to predict turbulence enhancement and dependence of pressure drop on gas velocity at high Reynolds numbers. Particle Reynolds number is directly proportional to the slip velocity between the gas and solid phases. It is hypothesized that as the particle Reynolds number increases, the difference between the velocities of the two phases increases, and the perturbation in gas motion behind the moving particles results in turbulence enhancement of the gas phase. The existing model does not account for this increase in gas turbulence modulation, so further refinement will require the addition of models that consider the gas behavior in particle wakes at high particle Reynolds numbers.

Acknowledgment

We thank the NSF/IGERT Fellowship for Therapeutic and Diagnostic Devices (DGE-99-72770), National Science Foundation Graduate Research Fellowship, and The Dow Chemical Co. for funding this work.

Literature Cited

(1) Knowlton, T. M. Solids Transfer in Fluidized Systems. In *Gas Fluidization Technology*; Geldart, D., Ed.; John Wiley & Sons Ltd.: Chichester, 1986; pp 341−414.

(2) Rhodes, M. *Introduction to Particle Technology*; John Wiley & Sons Ltd.: Chichester, U.K., 1998.

(3) Konno, H.; Saito, S. Pneumatic Conveying of Solids Through Straight Pipes. *J. Chem. Eng. Jpn.* **1969**, *2*, 211.

(4) Singh, B. Analysis of Pressure Drop in Vertical Pneumatic Conveying. A Generalized Approach for Gas-Particle and Liquid-Particle Systems. *Powder Technol.* **1982**, *32*, 179.

(5) Rautiainen, A.; Stewart, G.; Poikolainen, V.; Sarkomaa, P. An Experimental Study of Vertical Pneumatic Conveying. *Powder Technol.* **1999**, *104*, 139.

(6) Hettiaratchi, K.; Woodhead, S.; Reed, A. Comparison Between Pressure Drop in Horizontal and Vertical Pneumatic Conveying Pipelines. *Powder Technol.* **1998**, *95*, 67.

(7) Namkung, W.; Cho, M. Pressure Drop in a Vertical Pneumatic Conveying of Iron Ore. *Ind. Eng. Chem. Res.* **2002**, *41*, 5316.

(8) Marcus, R.; Leung, L.; Klinzing, G.; Rizk, F. *Pneumatic Conveying of Solids*; Chapman and Hall: London, 1990.

(9) Klinzing, G. *Gas−Solid Transport*; McGraw-Hill: New York, 1981.

(10) Nieuwland, J. J.; Kuipers, J. A. M.; van Swaaij, W. P. M. An Engineering Model for Dilute Riser Flow. *Powder Technol.* **1997**, *90*, 115.

(11) Plasynski, S.; Klinzing, G.; Mathur, M. High-Pressure Vertical Pneumatic Transport Investigation. *Powder Technol.* **1994**, *79*, 95.

(12) Pelegrina, A. H. Analysis of Pneumatic Conveying of Particles. *Latin Am. Appl. Res.* **2002**, *32*, 91.

(13) Yang, W.-C. Correlations for Solid Friction Factors in Vertical and Horizontal Pneumatic Conveyings. *AIChE J.* **1974**, *20*, 605.

(14) Yang, W.-C. A Correlation for Solid Friction Factor in Vertical Pneumatic Conveying Lines. *AIChE J.* **1978**, *24*, 548.

(15) Wang, F.-J.; Zhu, J.-X.; Beeckmans, J. M. Pressure Gradient and Particle Adhesion in the Pneumatic Transport of Cohesive Fine Powders. *Int. J. Multiphase Flow* **2000**, *26*, 245.

(16) Capes, C. E.; Nakamura, K. Vertical Pneumatic Conveying: An Experimental Study with Particles in the Intermediate and Turbulent Flow Regimes. *Can. J. Chem. Eng.* **1973**, *51*, 31.

(17) Pettyjohn, E. S.; Christiansen, E. B. Effect of Particle Shape on Free-Settling Rates of Isometric Particles. *Chem. Eng. Prog.* **1948**, *44*, 157.

(18) Clift, R.; Grace, J. R.; Weber, M. E. *Bubbles, Drops, and Particles*; Academic Press: New York, 1978.

(19) Hariu, O. H.; Molstad, M. C. Pressure Drop in Vertical Tubes in Transport of Solids by Gases. *Ind. Eng. Chem. Res.* **1949**, *41*, 1148.

(20) Haider, A.; Levenspiel, O. Drag Coefficient and Terminal Velocity of Spherical and Nonspherical Particles. *Powder Technol.* **1989**, *58*, 63.

(21) Arastoopour, H.; Gidaspow, D. Vertical Pneumatic Conveying using Four Hydrodynamic Models. *Ind. Eng. Chem. Fundam.* **1979**, *18*, 123.

(22) Nakamura, K.; Capes, C. A Theoretical Study of Uniform and Annular Particle Flow Models. *Can. J. Chem. Eng.* **1973**, *51*, 39.

(23) Chen, H.; Marshall, J. S. A Lagrangian Vorticity Method for Two-Phase Particulate Flows with Two-Way Phase Coupling. *J. Comput. Phys.* **1999**, *148*, 169.

(24) Sinclair, J. L.; Jackson, R. Gas-Particle Flow in a Vertical Pipe with Particle−Particle Interactions. *AIChE J.* **1989**, *35*, 1473.

(25) Anderson, T.; Jackson, R. A Fluid Mechanical Description of Fluidized Beds. *Ind. Eng. Chem. Fundam.* **1967**, *6*, 527.

(26) Louge, M.; Mastorakos, E.; Jenkins, J. The Role of Particle Collisions in Pneumatic Transport. *J. Fluid Mech.* **1991**, *231*, 345.

(27) Bolio, E.; Yasuna, J.; Sinclair, J. Dilute Turbulent Gas−Solid Flow in Risers with Particle−Particle Interactions. *AIChE J.* **1995**, *41*, 1375.

(28) Lun, C.; Savage, S. Kinetic Theory for Rapid Flow. Department of Civil Engineering and Applied Mechanics, McGill University, Canada, 1987, unpublished manuscript.

(29) Hadinoto, K.; Curtis, J. S. Effect of Interstitial Fluid on Particle−Particle Interactions in Kinetic Theory Approach of Dilute Turbulent Fluid-Particle Flow. *Ind. Eng. Chem. Res.* **2004**, submitted for publication.

(30) Henthorn, K. Measurement and Prediction of Particle Entrainment and Conveying: Effect of Particle Characteristics, Mass Loading, and Reynolds Number. Ph.D. Dissertation, Purdue University, West Lafayette, IN, 2004.

(31) Goldsmith, W. *Impact: The Theory and Physical Behaviour of Colliding Solids*; Richard Clay and Co. Ltd.: London, 1960.

(32) Gondret, P.; Lance, M.; Petit, L. Bouncing Motion of Spherical Particles in Fluids. *Phys. Fluids* **2002**, *14*, 643.

(33) Sinclair, J.; Mallo, T. Describing Particle-Turbulence Interaction in a Two-Fluid Modeling Framework. *Proceedings of FEDSM'98: 1998 ASME Fluids Engineering Division Summer Meeting*, Washington, DC, June 21−25, 1998; ASME Press: New York, 1998; Vol. 4, pp 7−14.

(34) Hadinoto, K.; Yurteri, C.; Curtis, J. Reynolds number effect on gas-phase turbulence in gas-particle flows: particle size effect. *Int. J. Multiphase Flow* **2004**, submitted for publication.

(35) Tsuji, Y.; Morikawa, Y.; Shiomi, H. LDV Measurements of an Air-Solid Two-Phase Flow in a Vertical Pipe. *J. Fluid Mech.* **1984**, *139*, 417.

(36) Lee, S. L.; Durst, F. On the Motion of Particles in Turbulent Duct Flows. *Int. J. Multiphase Flow* **1982**, *8*, 125.

(37) Lun, C.; Savage, S.; Jeffrey, D.; Chepurniy, N. Kinetic Theories for Granular Flow; Inelastic Particles in Couette Flow and Slightly Inelastic Particles in a General Flow Field. *J. Fluid Mech.* **1984**, *140*, 223.

(38) Huthmann, M.; Aspelmeier, T.; Zippelius, A. Granular Cooling of Hard Needles. *Phys. Rev. E* **1999**, *60*, 654.

(39) Aspelmeier, T.; Huthmann, M.; Zippelius, A. Free Cooling of Particles with Rotational Degrees of Freedom. *Lecture Notes in Physics: Granular Matter*; Springer: Berlin, 2000.

(40) Walton, O.; Braun, R. Simulation of Rotary-Drum and Repose Tests for Frictional Spheres and Rigid Sphere Clusters. Joint DOE/NSF Workshop on Flow of Particulates and Fluids, Ithaca, NY, 1993.

Received for review June 7, 2004
Revised manuscript received August 24, 2004
Accepted August 30, 2004

IE049505E